


# Tuber Locations Associated with Infantile Spasms Map to a Common Brain Network



Alexander L. Cohen, MD, PhD <sup>1,2,3</sup> Brechtje P. F. Mulder, BSc,<sup>1,4</sup> Anna K. Prohl, BA,<sup>2</sup>

Louis Soussand, MS <sup>3</sup> Peter Davis, MD,<sup>1</sup> Mallory R. Kroeck, MA,<sup>1,2,3</sup>

Peter McManus, BA,<sup>1,2,3</sup> Ali Gholipour, PhD <sup>2</sup> Benoit Scherrer, PhD <sup>2</sup>

E. Martina Bebin, MD, MPA,<sup>5</sup> Joyce Y. Wu, MD,<sup>6</sup> Hope Northrup, MD,<sup>7</sup>

Darcy A. Krueger, MD, PhD <sup>8</sup> Mustafa Sahin, MD, PhD <sup>1,9</sup> Simon K. Warfield, PhD <sup>2</sup>

Michael D. Fox, MD, PhD <sup>3,10,11†</sup> Jurriaan M. Peters, MD, PhD, <sup>1,2†</sup>

and for the Tuberous Sclerosis Complex Autism Center of Excellence Network Study Group

**Objective:** Approximately 50% of patients with tuberous sclerosis complex develop infantile spasms, a sudden onset epilepsy syndrome associated with poor neurological outcomes. An increased burden of tubers confers an elevated risk of infantile spasms, but it remains unknown whether some tuber locations confer higher risk than others. Here, we test whether tuber location and connectivity are associated with infantile spasms.

**Methods:** We segmented tubers from 123 children with ( $n = 74$ ) and without ( $n = 49$ ) infantile spasms from a prospective observational cohort. We used voxelwise lesion symptom mapping to test for an association between spasms and tuber location. We then used lesion network mapping to test for an association between spasms and connectivity with tuber locations. Finally, we tested the discriminability of identified associations with logistic regression and cross-validation as well as statistical mediation.

**Results:** Tuber locations associated with infantile spasms were heterogeneous, and no single location was significantly associated with spasms. However, >95% of tuber locations associated with spasms were functionally connected to the globi pallidi and cerebellar vermis. These connections were specific compared to tubers in patients without spasms. Logistic regression found that globus pallidus connectivity was a stronger predictor of spasms (odds ratio [OR] = 1.96, 95% confidence interval [CI] = 1.10–3.50,  $p = 0.02$ ) than tuber burden (OR = 1.65, 95% CI = 0.90–3.04,  $p = 0.11$ ), with a mean receiver operating characteristic area under the curve of 0.73 ( $\pm 0.1$ ) during repeated cross-validation.

**Interpretation:** Connectivity between tuber locations and the bilateral globi pallidi is associated with infantile spasms. Our findings lend insight into spasm pathophysiology and may identify patients at risk.

ANN NEUROL 2021;89:726–739

View this article online at [wileyonlinelibrary.com](http://wileyonlinelibrary.com). DOI: 10.1002/ana.26015

Received Apr 14, 2020, and in revised form Jan 4, 2021. Accepted for publication Jan 4, 2021.

Address correspondence to Dr Cohen, Department of Neurology, Boston Children's Hospital, 300 Longwood Avenue, Boston, MA 02115.

E-mail: [alexander.cohen2@childrens.harvard.edu](mailto:alexander.cohen2@childrens.harvard.edu)

<sup>†</sup>M.F. and J.M.P. share senior authorship.

From the <sup>1</sup>Department of Neurology, Boston Children's Hospital, Harvard Medical School, Boston, MA; <sup>2</sup>Computational Radiology Laboratory, Department of Radiology, Boston Children's Hospital, Harvard Medical School, Boston, MA; <sup>3</sup>Laboratory for Brain Network Imaging and Modulation, Berenson-Allen Center for Noninvasive Brain Stimulation and Division of Cognitive Neurology, Department of Neurology, Beth Israel Deaconess Medical Center, Harvard Medical School, Boston, MA; <sup>4</sup>VUmc School of Medical Sciences, VU University Medical Center Amsterdam, Amsterdam, the Netherlands; <sup>5</sup>Department of Neurology, University of Alabama at Birmingham, Birmingham, AL; <sup>6</sup>Division of Pediatric Neurology, UCLA Mattel Children's Hospital, David Geffen School of Medicine, University of California, Los Angeles, Los Angeles, CA; <sup>7</sup>Division of Medical Genetics, McGovern Medical School, University of Texas Health Science Center at Houston, Houston, TX; <sup>8</sup>Department of Neurology, Cincinnati Children's Hospital Medical Center, Cincinnati, OH; <sup>9</sup>F. M. Kirby Neurobiology Center, Boston Children's Hospital, Harvard Medical School, Harvard University, Boston, MA; <sup>10</sup>Athinoula A. Martinos Center for Biomedical Imaging, Department of Radiology, Massachusetts General Hospital, Charlestown, MA; and <sup>11</sup>Department of Neurology, Massachusetts General Hospital, Harvard Medical School, Boston, MA

Additional supporting information can be found in the online version of this article.

**T**uberous sclerosis complex (TSC) is a neurogenetic disorder with an incidence of 1 in 6,000 live births<sup>1</sup> resulting from pathogenic variants in either the *TSC1* or *TSC2* gene. TSC is characterized by overactivation of the mechanistic target of rapamycin pathway leading to abnormalities in cell growth, differentiation, and migration, which cause the formation of macroscopic lesions in the brain, including tubers, radial migration lines, and subependymal nodules. In particular, tubers demonstrate aberrant cortical lamination and contain poorly differentiated cells with an ambiguous neuronal–glial phenotype akin to focal cortical dysplasia type IIb.<sup>2</sup> Tubers are potentially epileptogenic and in cases of refractory epilepsy in TSC patients, often represent the target of epilepsy surgery.<sup>3</sup>

Approximately 50% of children with TSC develop infantile spasms, a rapid onset early childhood epilepsy syndrome that typically occurs in the first year of life as clusters of generalized flexor or extensor spasms,<sup>4,5</sup> and can occur with numerous structural, metabolic, and genetic etiologies.<sup>6</sup> Because tubers are thought to disrupt local cortical architecture, others have studied whether tuber distribution can predict specific neurological phenotypes, including infantile spasms.<sup>7–9</sup> Unfortunately, these associations have not been consistently replicated across cohorts.<sup>10–12</sup> A recent study of non-TSC-related infantile spasms found that early acquired brain injury to deep gray matter nuclei may be associated with an increased risk for infantile spasms<sup>13</sup>; however, a consistent and reproducible pattern of lesion locations that leads to infantile spasms has not yet been found.<sup>8,9,14</sup> Furthermore, the pathophysiology of how focal lesions result in generalized epileptic spasms remains unknown.<sup>13</sup> As such, there is a knowledge gap in understanding whether specific patterns of cerebral involvement are associated with infantile spasms.

One approach to linking lesion location and symptom expression is voxelwise lesion symptom mapping, typically used to study clinical syndromes in acute stroke.<sup>15</sup> When lesion locations across patients with similar symptoms overlap, neurological symptoms can be attributed to specific brain regions. Although tuber burden and qualitative tuber location have been examined, formal voxelwise lesion symptom mapping of tubers for specific symptoms in TSC has not yet been explored, likely due to the need for larger sample sizes and computer-aided lesion delineation.<sup>8,9,14</sup>

It is possible, however, that infantile spasms result from injury to a specific network, as opposed to dysfunction of a single region. Lesion network mapping identifies the network of brain regions connected to each lesion location using a normative map of functional connectivity.<sup>16</sup> Connections associated with a specific symptom can then be identified. This technique has been successfully used to elucidate lesion-induced hallucinations, delusions,

movement disorders, and a variety of other symptoms,<sup>16–20</sup> and lesion network mapping results have shown promise as treatment targets for therapeutic brain stimulation.<sup>21</sup> Here, we identified tuber distributions from a large cohort of patients with TSC and applied both traditional voxelwise lesion symptom mapping and more novel lesion network mapping to determine whether there is a spasmogenic network that is critical to the generation of infantile spasms.

## Patients and Methods

### Patients

Patients' data were obtained from the Tuberous Sclerosis Complex Autism Center of Excellence Network (TACERN) multicenter prospective study (NIH U01 NS082320).<sup>4</sup> Patients were enrolled in the first year of life and followed longitudinally through 36 months of age. Informed consent was obtained for each patient, as approved by the institutional review board at each participating site. Inclusion criteria for the current study included availability of high-quality structural neuroimaging demonstrating visibly present cortical tubers.

### Tuber Segmentation and Coregistration

Each patient's T1-weighted (T1w) structural magnetic resonance imaging (MRI) was processed as previously described.<sup>2</sup> As tubers show minimal evolution in location and volume on imaging,<sup>2</sup> the highest contrast MRI (at age > 2 years) was used. An automated lesion segmentation algorithm<sup>22</sup> was trained on 20 manually segmented T1w, T2w, and fluid-attenuated inversion recovery MRI images of children with TSC and validated on images from an additional 10 children, all of whom were not patients in the present study. This algorithm was then applied to each patient's neuroimaging, followed by visual inspection and manual correction of all tuber segmentations with ITK-SNAP.<sup>23</sup> In all cases, the final delineation of tuber distributions was subject to experienced expert review (J.M.P.). All identified tuber voxels for each participant were coded equally, that is, not segmented into separable tubers. We then registered each patient's tuber distribution to a common space using the MNI152 2009c nonlinear asymmetric template and Advanced Normalization Tools software, which allows "unweighting" of lesion locations.<sup>24</sup>

### Voxelwise Lesion Symptom Mapping of Tuber Distributions Associated with Infantile Spasms

We performed voxelwise lesion symptom mapping to identify relationships between specific tuber location and infantile spasms.<sup>15,25</sup> At each voxel affected by at least 3 tubers across the 123 patients,<sup>26</sup> the association of tuber

presence and infantile spasms was tested via Lieberman test, using permutation-based voxelwise statistics controlling for familywise error with NiiStat.<sup>25</sup> To account for the spatial dependence between adjacent voxels, a whole-brain Bayesian spatial generalized linear mixed model<sup>27</sup> was used to determine the probability of tuber presence in patients with and without infantile spasms.

### **Quantitative Assessment of Overall Tuber Location and Burden**

Lobar and overall cortical gray matter burden was calculated using masks created from the MNI probabilistic structural atlas distributed with FMRIB Software Library (FSL)<sup>28</sup> (thresholded at 15). A 2-way analysis of variance (ANOVA) assessed for main effect of group, main effect of lobe, and group  $\times$  lobe interaction (www.R-project.org). To compare with prior work assessing the presence or absence of tubers in particular lobes, we also calculated the percentage of patients with lobar involvement  $>0.5\%$ , omitting lobes with minimal tuber pathology.

### **Lesion Network Mapping of Tuber Distributions Associated with Infantile Spasms**

The tuber segmentation from each patient with infantile spasms was used as a seed in a resting-state functional connectivity analysis of data collected from 1,000 healthy young adult controls,<sup>29</sup> similar to prior studies,<sup>16–21</sup> creating a T map for each patient where the value of each voxel represents the functional connectivity between that voxel and segmented tubers. Each patient's T map was then thresholded ( $T > \pm 11$ , voxelwise familywise error [FWE] corrected at  $p < 10^{-12}$ ) to create a binarized map of regions strongly functionally connected to each patient's tuber distribution. The overlap of these maps identified voxels consistently functionally connected to tubers. A clustering algorithm (Nilearn connected\_regions<sup>30</sup>) was used to identify regions of interest (ROIs) of  $>50\text{mm}^3$  that were  $>95\%$  sensitive for infantile spasms. To maximize the spatial specificity of our localization, a threshold of  $T > \pm 11$  was utilized; using thresholds of  $T > \pm 9$  or 7 did not change the interpretation of our results,<sup>31</sup> and all statistical analyses described below used continuous values that did not depend on a threshold/cutoff.

### **Split-Half Replication of Lesion Network Mapping Results**

To assess the reliability of our lesion network overlap results, we divided our infantile spasms cohort into 2 subsets of 37 patients each. We then repeated the above lesion network mapping on each subset and connected regions derived using the same T score threshold as above.

As such, this represented a test of the sensitivity of the overlap procedure across patients with infantile spasms.

### **Specificity of Tuber Distribution Connectivity for Infantile Spasms**

We also assessed the specificity of functional connectivity patterns for infantile spasms as in prior lesion network mapping studies.<sup>16–21</sup> A voxelwise 2-sample  $t$  test was performed via permutation testing (FSL PALM v.alpha109) using 2,000 permutations, tail approximation,<sup>25</sup> and a voxelwise FWE-corrected  $p < 0.05$ . Permutation testing and voxelwise statistics were chosen because they are more resilient to the false positives seen with cluster-based approaches.<sup>32</sup>

### **Identifying Connections and Tuber Locations Both Sensitive and Specific to TSC-Associated Infantile Spasms**

We next identified regions that were both sensitive and specific for infantile spasms, that is, the conjunction of voxels functionally connected to 95% of tuber distributions causing infantile spasms and demonstrating statistically stronger connectivity to tubers in patients with infantile spasms versus without. We also used these regions as functional connectivity seeds to perform an inverse mapping, that is, defining the brain network that best encompasses tubers uniquely associated with infantile spasms. Although circular, this allows for visual inspection of which individual tuber or set of tubers in any given patient may be most likely to be driving the association with infantile spasms.

### **Replication of Lesion Network Mapping Results across Genetic Diagnoses**

Because *TSC2* gene mutation is often associated with a more severe phenotype, we tested whether the patterns seen in the overall cohort depended on genetic diagnosis by repeating the above permutation-based 2-sample  $t$  test with genetic diagnosis included as a covariate and by performing both the lesion network overlap and statistical testing separately in genetically consistent subsamples. For the latter, we generated a cohort of 76 patients with confirmed *TSC2* gene mutations (47 with infantile spasms) and a cohort of the remaining 47 patients with either *TSC1* gene mutations or indeterminate gene mutations (27 with infantile spasms).

### **Replication of Lesion Network Mapping Results with Pediatric Functional Connectome Data**

To assess the consistency of our findings with pediatric connectivity data, we repeated the analyses above using data from the Adolescent Brain Cognitive Development (ABCD) study of 10,000 9–10-year-old participants,

which recently became available in National Institute of Mental Health Data Archive Collection #3165 ([https://nda.nih.gov/edit\\_collection.html?id=3165](https://nda.nih.gov/edit_collection.html?id=3165)).<sup>33</sup> This represents the “youngest” large-scale normative functional connectivity data currently available. A cohort of 1,000 participants were identified with parameters consistent with our young adult connectome,<sup>31</sup> that is, acquired on Siemens (Erlangen, Germany) MRI scanners, without reported Diagnostic and Statistical Manual of Mental Disorders, 5th edition criteria diagnoses or traumatic brain injury, and with low in-scanner movement. The latter was approximated via the number of resting state functional MRI (rs-fMRI) time points below a framewise displacement threshold of 0.2. Preprocessing of this ABCD cohort was performed using FreeSurfer7.1<sup>34</sup> and a modified version of the Computational Brain Imaging Group functional connectivity preprocessing pipeline<sup>35</sup> (<https://github.com/bchcohenlab>) that more closely reflects the preprocessing of the original young adult cohort.<sup>29</sup> Lesion network mapping and specificity analyses were then performed as described above. Due to differences in statistical power of the connectivity patterns seen in the ABCD dataset with the current processing pipeline, a  $T$  threshold of  $T > \pm 9$  (voxelwise FWE corrected at  $p < 10^{-12}$ ) appeared to be most similar to a  $T > \pm 11$  in the young adult connectome.

### Identifying Independent Predictors of Infantile Spasms with Logistic Regression

We modeled the binary outcome of infantile spasms using logistic regression with the Statsmodels Python package.<sup>36</sup> The models related infantile spasms to the independent variables of tuber-to-identified ROI correlations and tuber burden for our 123 patients. Odds ratios (ORs), 95% confidence intervals (CIs), McFadden pseudo  $R^2$ , and Akaike information criterion were then computed.

### Consistency Testing via Repeated Stratified K-Fold Cross-Validation

We used cross-validation to test the internal reproducibility of predicting infantile spasms based on our findings. Using the logistic regression model that best described the data, we performed a repeated stratified K-fold cross-validation using Scikit-learn,<sup>37</sup> iteratively training a model using 80% of the 123 patients, maintaining the relative ratio of patients with and without spasms. This model was then used to classify the remaining 20%. The classification results of 5,000 iterations, with random shuffling within groups, was used to create receiver operating characteristic curves. We then calculated the mean area under the curve and the variance of the curve when differing subsets of the data are used. Distinct from the split-half replication

above, this analysis tests the consistency of the difference between patients with and without infantile spasms.

### Assessing for Mediation of the Relationships between Independent Predictors and Infantile Spasms

Finally, we performed a statistical mediation analysis<sup>38</sup> using the SPSS PROCESS macro<sup>39</sup> to determine whether the identified relationship between independent predictors and infantile spasms were a byproduct of statistical mediation. In other words, does  $X$  predict  $Y$  ( $X \rightarrow Y$ ) solely or in part because  $X$  predicts  $M$ , which in turn predicts  $Y$  ( $X \rightarrow M \rightarrow Y$ ). Reverse models were also assessed to be agnostic in regard to the directionality of mediation. Five thousand bootstrap samples were used to calculate significance of the indirect pathway via CIs.

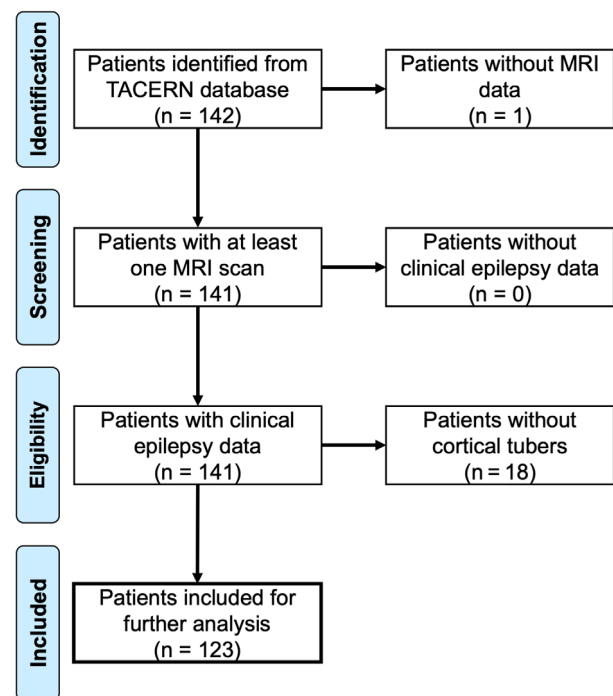


**FIGURE 1: PRISMA flow chart identifying Tuberous Sclerosis Complex Autism Center of Excellence Network (TACERN) research patients with and without infantile spasms.** Patients were identified from the prospective TACERN cohort study of children with tuberous sclerosis complex. Inclusion criteria included availability of neuroimaging data of sufficient quality to identify tubers, sufficient clinical follow-up to accurately delineate patients who did or did not develop infantile spasms, and the presence of identifiable tubers on neuroimaging so that tuber locations could be used for lesion network mapping. One hundred twenty-three patients met these criteria, whereas 19 were excluded, due to either the lack of available neuroimaging or the absence of detectable tubers. MRI = magnetic resonance imaging.

## Results

### Patient Demographics

We identified 142 children who completed all study visits with clinical and/or genetic criteria for definite TSC from the prospective multicenter TACERN dataset.<sup>4</sup> Nineteen patients were excluded due to either a lack of available neuroimaging ( $n = 1$ ) or a lack of visibly present tubers on neuroimaging ( $n = 18$ , 3 of whom had infantile spasms). During study follow-up through 3 years of age, 74 patients developed infantile spasms, whereas 49 patients did not (Fig 1). The two groups were largely similar in regard to sex (47% male vs 57%) and age at time of neuroimaging (2.74 vs 2.53 years old). We found a higher prevalence of infantile spasms in patients with a *TSC2* gene mutation compared to those with a *TSC1* gene mutation (67% vs 21%,  $p = 0.012$ ), consistent with prior work<sup>4</sup> (Table 1). As expected, all patients who developed infantile spasms received antiepileptic agents after the development of

spasms, consistent with standard recommendations. Of note, 13 patients who developed infantile spasms (17.6%) received antiepileptic medications prior to the onset of infantile spasms to treat other semiologies. Of these, only levetiracetam ( $n = 9$ ) was used in more than 3 patients. Conversely, 28 patients (57.1%) who did not develop infantile spasms received antiepileptic medications for other semiologies. If this treatment prevented the development of infantile spasms in a proportion of patients, this would have created bias against the findings presented below and thus does not represent a limitation.

### Distribution of Tubers in TSC

The number and spatial location of tubers was highly heterogeneous across patients (Fig 2). The median tuber burden for our entire cohort was 2.10% of the cortical gray matter (24.7 cm<sup>3</sup>; see Table 1). Tubers were largely stochastically distributed across the brain (Fig 3A). Although

**TABLE 1. Patient Demographics and Tuber Distribution**

	Spasms+	Spasms—	Total
Patients, n	74	49	123
Male sex, n (%)	35 (47)	28 (57)	63 (51)
Mean age at scan, yr (range)	2.74 (0.76–5.44)	2.53 (0.32–3.89)	2.66 (0.32–5.44)
Mean age at spasm onset, days (range)	168 (0–519)	n/a	n/a
Genotype, n (% of total)			
<i>TSC1</i> mutation	4 (27.7)	11 (73.3)	15 (100)
<i>TSC2</i> mutation	47 (61.8)	29 (38.2)	76 (100)
No mutation identified	7 (58.3)	5 (41.7)	12 (100)
Unknown	16 (80.0)	4 (20.0)	20 (100)
Median tuber burden, % (25–75% range)			
All cortical gray matter	2.59 (1.58–4.73)	0.85 (0.08–2.34)	2.10 (0.69–3.76)
Frontal lobe	2.91 (1.50–4.78)	1.04 (0.06–2.66)	2.17 (0.71–4.48)
Parietal lobe	2.31 (1.33–4.17)	0.95 (0.05–2.76)	1.68 (0.29–3.33)
Temporal lobe	1.99 (0.87–5.35)	0.42 (0.04–2.32)	1.44 (0.19–3.89)
Occipital lobe	1.90 (0.87–3.55)	0.88 (0.00–2.03)	1.54 (0.24–2.99)
Tuber frequency, %			
Frontal lobe	92	59	79
Parietal lobe	85	53	72
Temporal lobe	81	47	67
Occipital lobe	84	53	72

n/a = not applicable.

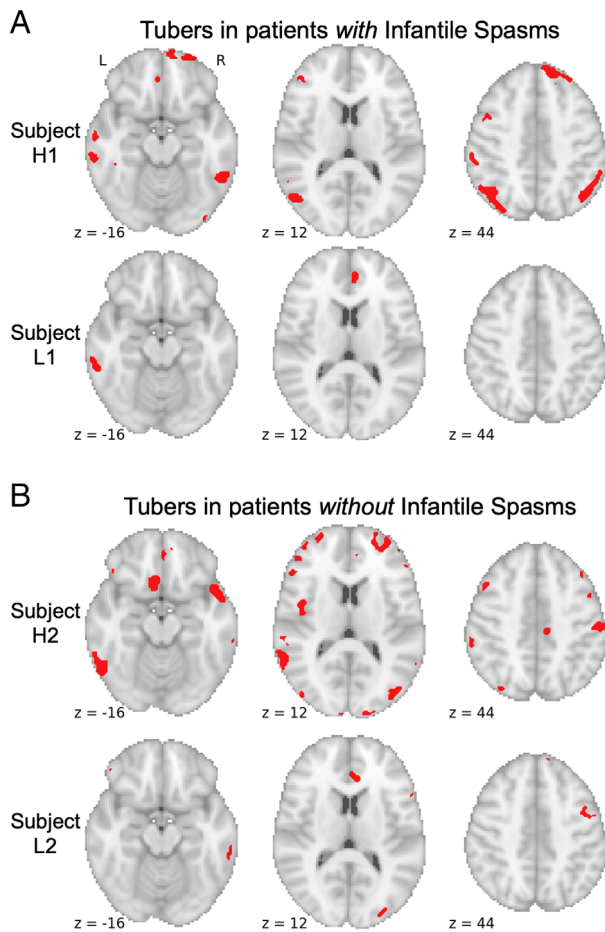


**FIGURE 2: Sample tuber distributions from children with and without a history of infantile spasms.** Tubers were segmented from all 123 children using a semiautomated approach and registered to a common brain atlas (Montreal Neurological Institute 6th generation atlas). Example tuber distributions are shown in red from the 74 children with infantile spasms (A) and the 49 children without infantile spasms (B), demonstrating that both groups included children with high tuber burdens (Participants H1 and H2) as well as low tuber burdens (Participants L1 and L2) that could not be visibly distinguished from one another.

visual inspection suggested a relative sparing of primary motor and visual cortices, this pattern was not statistically significant when assessed using *a priori* parcellations, nor did this differentiate between patients with and without infantile spasms (see Fig 3B, C).

### Association of Tuber Locations with a History of Infantile Spasms

No single brain region was affected by tubers in all cases of infantile spasms. The maximum overlap of tuber locations across the cohort with spasms was only 24.3% (18/74 patients). Voxelwise lesion symptom mapping failed to identify any significant associations between tuber location and infantile spasms, and the highest predictive

value of any location for infantile spasms was 24% (see Fig 3D). Although overall tuber burden was higher in patients with infantile spasms than in those without (2-way ANOVA 2.59% vs 0.85%,  $p < .0001$ ), there was no significant difference across different brain lobes ( $p = 0.144$ ; see Fig 3E, F, Table 1).

### Lesion Network Mapping of Tubers in TSC Patients with Infantile Spasms

The network of brain regions functionally connected to each patient's tuber locations was computed (Fig 4A, B), and connections common to >95% of the 74 patients with infantile spasms were identified (see Fig 4C). Both left and right internal segments of the globi pallidi and the cerebellar vermis (lobule VIIIA) demonstrated consistent negative functional connectivity with tuber distributions associated with infantile spasms. Peak voxelwise overlap was seen in 72 of 74 patients in the right globus pallidus, 73 of 74 in the left globus pallidus, and 74 of 74 in the cerebellar vermis. Split-half replication demonstrated consistent localization of this overlap across independent subgroups (see Fig 4D). Repeating this analysis solely for patients with *TSC2* mutations ( $n = 47$ ) and solely for patients with either confirmed *TSC1* or indeterminate mutations ( $n = 27$ ) both also identified consistent localization to the bilateral globi pallidi and cerebellar vermis. Performing lesion network mapping on the tuber distributions from the 49 children without infantile spasms did not reveal any consistently connected regions.

### Specificity of Lesion Network Connectivity Patterns for Infantile Spasms

A voxelwise permutation-based 2-sample *t* test was used to compare lesion network maps of patients with versus without infantile spasms, controlling for genetic diagnosis as a covariate. Negative connectivity to the bilateral globi pallidi and cerebellar vermis was highly specific to patients with versus without infantile spasms (FWE corrected  $p < 0.05$ ) and was not driven by the higher incidence of infantile spasms among patients with *TSC2* gene mutations noted above.<sup>4</sup> The conjunction of a mask of these significant voxels and the lesion network mapping analysis above generated a map of regions both sensitive and specific for infantile spasms (see Fig 4E).

### Replication of Lesion Mapping Results with Pediatric Functional Connectome Data

Repeating the above analyses using a pediatric normative connective (1,000 9-year-old participants from the ABCD study) identified consistent connectivity patterns. Regions were again identified in the left and right globus pallidus, with peak voxelwise overlap of 63 of 74 in each and 65 of



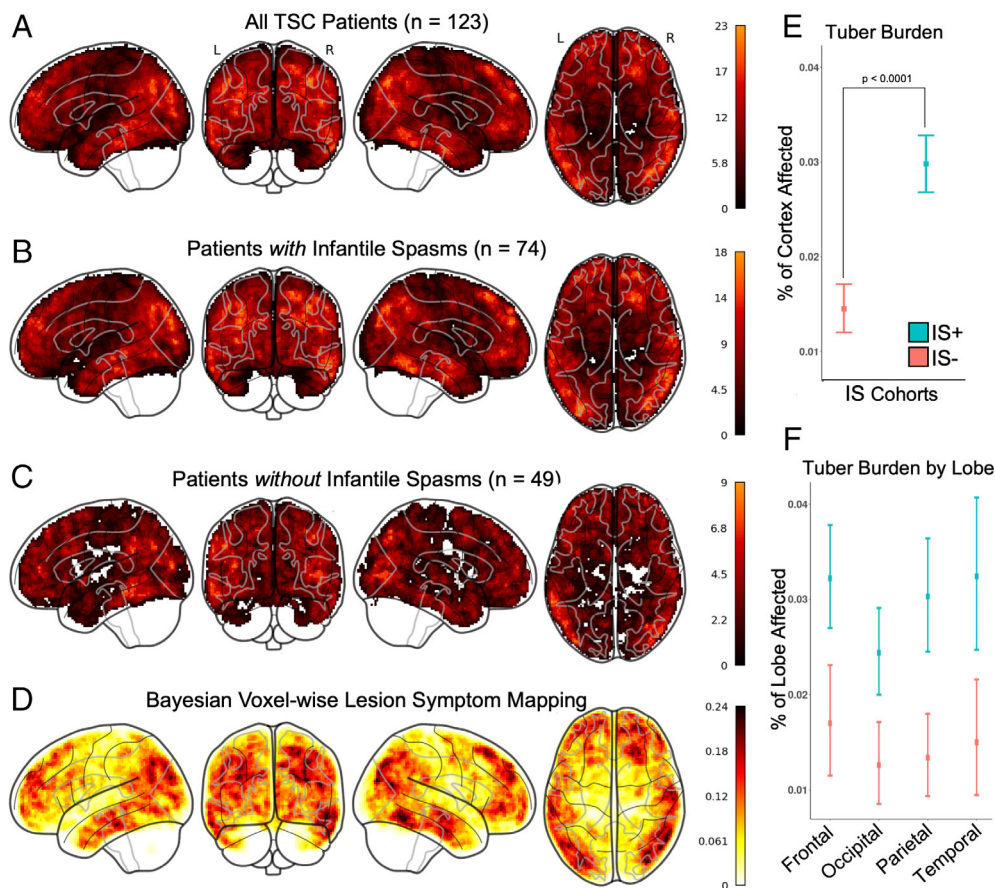


**FIGURE 3:** Increased tuber burden, but not tuber location, is associated with infantile spasms (IS). Binary tuber distribution masks were summed for all children with tuberous sclerosis complex (TSC; A), the cohort of children with IS (B), and the cohort of children without IS (C). Both visual comparison and quantitative spatial analysis (D) did not identify a particular pattern for tuber distribution in general, nor that distinguished between children with and without a history of infantile spasms. Whereas overall tuber burden was statistically different between the two cohorts (E), there was not a statistically significant difference between cortical lobe involvement (F).

74 in the cerebellar vermis. A 2-sample  $t$  test was again computed as above, and the intersection of these regions with a mask of significant voxels (uncorrected  $p < 0.005$ ) was again computed to identify regions both sensitive and specific for infantile spasms (see Fig 4F).

### Tuber Locations Most Likely to be Associated with Infantile Spasms

A map was created from the intersection of regions with both strong negative connectivity to the globi pallidi and strong negative connectivity to the cerebellar vermis (Fig 5A). This defined a specific brain network that best encompasses tuber locations associated with infantile spasms. Comparison of the tuber distributions from patients with and without infantile spasms (see Fig 5B, C) demonstrates a higher proportion of tuber–network overlap in patients with infantile spasms (see Fig 5B, blue circles), even in patients with low tuber burden (eg, Participant L1 vs Participant L2).

### Evaluating Independent Predictors of Infantile Spasms

Tuber burden, globus pallidus connectivity, and cerebellar vermis connectivity were each separately associated with infantile spasms (Table 2, Models 1–3). However, in combined models that included connectivity to the globi pallidi, all other independent variables became nonsignificant (see Table 2, Models 4–6). A model relating tuber burden and globus pallidus connectivity best represented the underlying data and explained the most variance (see Table 2, Model 5). In this model, globus pallidus connectivity was a stronger predictor of infantile spasms than tuber burden (OR = 1.96, 95% CI = 1.10–3.50,  $p = 0.02$  vs OR = 1.65, 95% CI = 0.90–3.04,  $p = 0.18$ ). Repeated stratified K-fold cross-validation of this model, using 80% of the 123 patients to train and testing for accuracy with the remaining 20%, was moderately accurate across 5,000 iterations, with a mean receiver operating characteristic area under the curve of 0.73 (standard deviation = 0.10; Fig 6A).

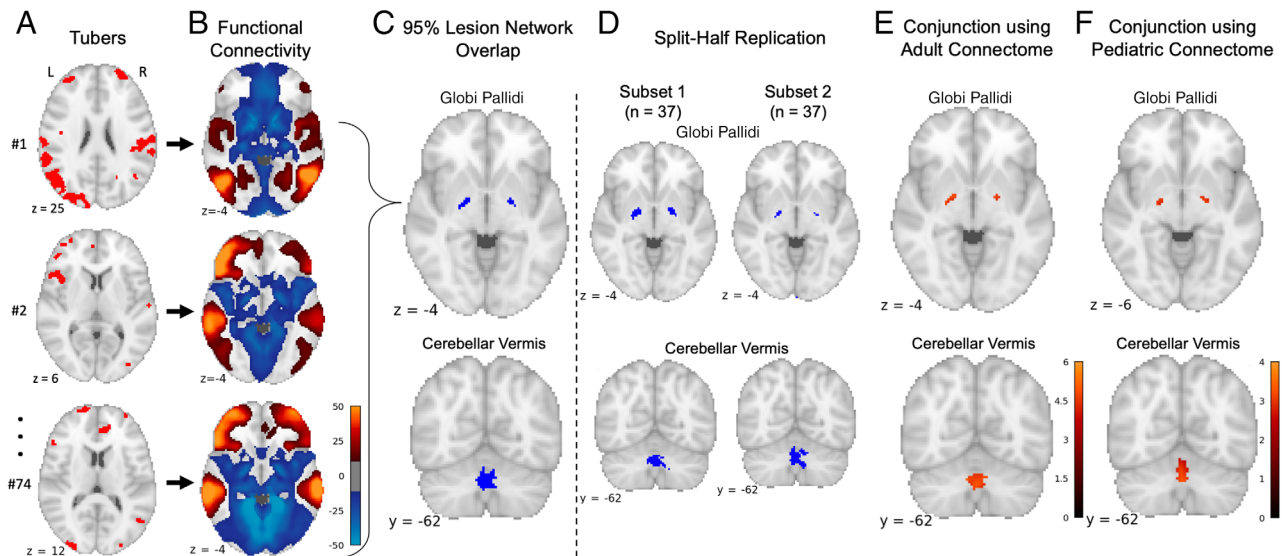


**FIGURE 4: Lesion network mapping identified 3 brain regions with consistent negative functional connectivity to tuber distributions associated with infantile spasms.** (A) The 74 tuber distributions associated with infantile spasms were registered to a standardized Montreal Neurological Institute brain template. (B) Brain regions functionally connected to each tuber distribution were identified using a large-scale functional connectivity database of young adult participants. (C) Overlap of these functional connectivity maps identified 3 brain regions connected to >95% of tuber distributions associated with infantile spasms: the left and right globus pallidus and the cerebellar vermis. (D) Consistent connected regions were also identified in 2 independent subsets. Of note, overlap of functional connectivity maps from the 49 children without infantile spasms did not reveal any consistently connected regions. Regions where connectivity was specific to infantile spasms were then identified by voxelwise 2-sample *t* test between children with infantile spasms and those without. (E) The conjunction of a mask of these significant voxels and the lesion network mapping analysis above generated a map of regions both sensitive and specific for infantile spasms, here shown controlling for genetic etiology as a covariate. (F) This process was repeated with an alternate large-scale functional connectivity database of 9-year-old participants identifying consistent results.

### Assessing for Mediation of the Relationships between Tuber Burden, Globus Pallidus Connectivity, and Infantile Spasms

A statistical mediation analysis found that the relationship between connectivity to the globi pallidi and infantile spasms was not the byproduct of increased tuber burden, that is, no mediation was detected (indirect effect: path  $ab = -0.306$ , boot standard error [SE] = 0.2091, 95% CI =  $-0.786$  to  $0.046$ ). However, the reverse model (see Fig 6B) found that the relationship between tuber burden and infantile spasms (path  $c$ ) was fully mediated by connectivity to the globi pallidi, that is, increased tuber burden predicts (path  $a$ ) increased connectivity to the globi pallidi, which in turn predicts (path  $b$ ) infantile spasms (indirect effect: path  $ab = 0.412$ , boot SE = 0.194, 95% CI =  $0.114$ – $0.872$ ). When this mediation is taken into account, tuber burden was no longer an independent predictor (path  $c'$ ) of infantile spasms, consistent with our logistic regression results (see Table 2).

### Discussion

In this large, prospectively acquired, and highly characterized TSC cohort derived from the TACERN study, we quantified the impact of tuber burden, location, and network involvement on infantile spasms. In line with

previously described cohorts, tuber burden was higher in patients with infantile spasms,<sup>14,40,41</sup> likely reflecting a more severe disease burden<sup>12,14,42</sup>; however, our results suggest a possible mechanism for this observation.

We found that tuber burden neither within particular lobes nor at specific locations across the brain were associated with infantile spasms. Instead, the distribution of tubers in children with infantile spasms defines a specific set of brain regions that is characterized by strong negative connectivity to the bilateral globi pallidi and cerebellar vermis. This finding was highly sensitive and specific to infantile spasms, was consistent across split-half replication, genetic etiology, and medication exposure, using a pediatric connectome to derive normative connectivity patterns, and demonstrated a stronger independent association with infantile spasms than tuber burden did alone.

These findings have 2 implications. First, network connectivity may explain why some children develop infantile spasms and others do not, through the convergence of anatomically variable lesions on a common pathway. This may also explain why increased tuber burden is also associated with spasms, as more tubers increase the likelihood that the identified network of brain regions is affected. Our mediation analysis suggests that increased



**TABLE 2. Family of Logistic Regression Models Identifying Globus Pallidus Connectivity as the Independent Variable Most Predictive of Infantile Spasms**

	Model 1	Model 2	Model 3	Model 4	Model 5	Model 6
Tuber volume						
OR (95% CI)	2.69 (1.60–4.50)	—	—	—	1.65 (0.90–3.04)	1.67 (0.88–3.15)
<i>p</i>	0.00017 <sup>a</sup>	—	—	—	0.11	0.12
Connectivity to the globi pallidi						
OR (95% CI)	—	2.68 (1.66–4.33)	—	2.37 (1.08–5.23)	1.96 (1.10–3.50)	2.21 (1.00–4.87)
<i>p</i>	—	0.000057 <sup>a</sup>	—	0.032 <sup>a</sup>	0.023 <sup>a</sup>	0.04978 <sup>a</sup>
Connectivity to the cerebellar vermis						
OR (95% CI)	—	—	2.27 (1.48–3.49)	1.15 (0.55–2.42)	—	0.95 (0.44–2.08)
<i>p</i>	—	—	0.00019 <sup>a</sup>	0.71	—	0.91
AIC	150.84	147.83	152.63	149.69	146.98	148.96
pseudo <i>R</i> <sup>2</sup>	0.112	0.130	0.101	0.131	0.148	0.148

<sup>a</sup>Statistically significant.  
AIC = Akaike information criterion; CI = confidence interval; OR = odds ratio.

connectivity between tuber locations and the globi pallidi may mediate the known association between tuber burden and infantile spasms; however, because the identification of globus pallidus connectivity as a predictor was also generated from this same dataset, hypothesis testing in this direction should be done with caution. Although there is increased excitability on a cellular level in TSC and increased epileptogenicity in brain tissue at and surrounding tubers, the basis of why infantile spasms are so prevalent in TSC, compared to other etiologies, is unknown.<sup>43</sup> Study of other lesional causes of infantile spasms, including early life stroke and periventricular leukomalacia, is needed to test whether the identified nodes in this pathway are consistent across causes of infantile spasms,<sup>6</sup> or whether they are unique to TSC.

Second, although more speculative, these findings lend further support to a proposed role for cortical–subcortical network interactions in the pathophysiology of infantile spasms.<sup>44</sup> Several converging lines of evidence suggest that the basal ganglia are a central “hub” in a spasmodic network affected by focal cortical lesions. Specifically, generalized epileptic spasms can resolve by surgical resection of singular focal structural lesions<sup>45</sup>; patients with congenital or early structural lesions that encompass the basal ganglia are at an increased risk for infantile

spasms<sup>13</sup>; and both positron emission tomography and electroencephalography (EEG)–functional MRI (fMRI) studies of infantile spasms have demonstrated extension of the epileptic network to the lenticular nuclei.<sup>46,47</sup>

Our results implicate the globi pallidi in the pathophysiology of infantile spasms, but the exact mechanism and whether the globi pallidi may represent a therapeutic target remain unknown. There is evidence that globus pallidus inhibition can lead to seizures in some scenarios but can lead to improved seizure control in others.<sup>48</sup> Although less is known about the role of the cerebellar vermis in epilepsy, it is involved in the corticoreticulocerebellar pathway to support movement generation and projects to the deep cerebellar nuclei, which have a hublike function for all output of the cerebellar network and an additional role in  $\gamma$ -aminobutyric acidergic (GABAergic) inhibition.<sup>49</sup> Furthermore, one of the most effective therapies for infantile spasms, vigabatrin, is an irreversible inhibitor of GABA aminotransferase, and although effective, can also lead to cytotoxic edema in the brain stem, dentate nuclei of the cerebellum, thalamus, and globi pallidi, consistent with their role in GABAergic metabolism and prominent concentration of GABAergic neurons.<sup>50–52</sup> Conversely, rodent models of infantile spasms often require simultaneous

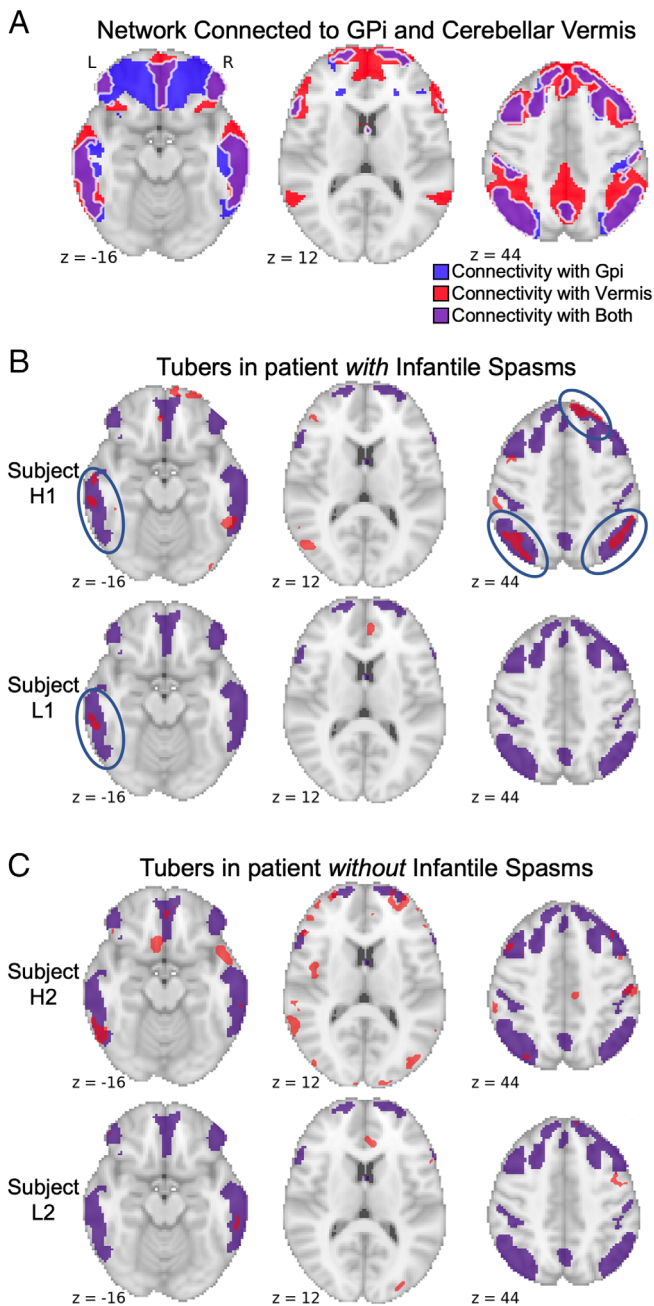


**FIGURE 5:** Lesion network connectivity with the bilateral globi pallidi and cerebellar vermis predicts locations where tubers are more likely to cause infantile spasms. (A) The intersection of connectivity with the globus pallidi (Gpi, blue shading) and connectivity with the cerebellar vermis (red shading) defined a specific network of areas (purple shading) predicted to be highly likely to cause infantile spasms if lesioned. (B, C) As a demonstration, the same 4 patients shown in Figure 2, 2 with infantile spasms and 2 without infantile spasms, and with either high or low tuber burden, are again shown here with tuber burden (in red) compared to the identified network (in purple). Among patients with infantile spasms (B), it can be seen that tubers are more likely to overlap with the predicted network (blue circles). Conversely, among patients without infantile spasms (C), tubers largely do not overlap with the predicted network.

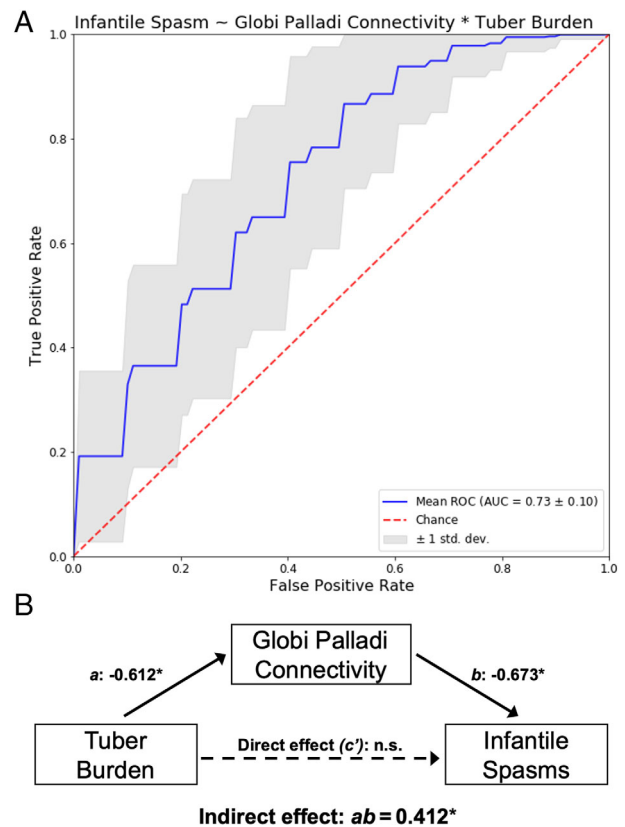


**FIGURE 6:** Logistic regression and statistical mediation analyses find that globus pallidus connectivity is a stronger predictor of infantile spasms than tuber burden and may mediate the observation that increased tuber burden is associated with infantile spasms. The performance of predicting infantile spasms from patients' tuber burden and globus pallidus connectivity (see Table 2, Model 5) was assessed using repeated stratified K-fold cross-validation. First, the 123 tuberous sclerosis complex patients were divided into 5 groups, then a logistic model was trained using 4 of these groups (ie, 80% of the data) and tested for accuracy on the remaining holdout group (ie, 20% of the data). (A) The classification results of 5,000 iterations of this process, with random shuffling within groups, was used to create receiver operating characteristic (ROC) curves. The mean ROC curve for this model is shown here (blue), along with a 1 standard deviation (std. dev.) cloud (gray) compared to chance (red). The area under the curve (AUC) was calculated to be 0.73 (std. dev. = 0.10). (B) A separate statistical mediation analysis identified that the relationship between tuber burden and infantile spasms (path c) is fully mediated by the serial relationship of tuber burden and globus pallidus connectivity (path a) and globus pallidus connectivity and infantile spasms (path b), with an indirect effect of path  $ab = 0.412$ , 95% confidence interval = 0.114–0.872. When this mediation is taken into account, tuber burden itself no longer independently predicts (path c') infantile spasms. Importantly, the reverse model found no mediation, that is, tuber burden does not mediate the relationship between globus pallidus connectivity and infantile spasms. n.s. = not significant.

injury to both cortical and subcortical structures including the thalamus and striatum.<sup>53</sup> We speculate that dysfunction of the globi pallidi or cerebellar vermis alone is not

sufficient to generate spasms and that increased cortical activity, in combination with failure of the modulating effects from these subcortical structures, culminates in infantile spasms.<sup>44</sup>

The finding that tuber locations are negatively correlated with the globi pallidi in children with infantile spasms means that as the fMRI signal at tuber locations goes up, the fMRI signal in the globi pallidi and cerebellar vermis goes down, and vice versa. However, the physiological interpretation of negative correlations, and the directionality of the interactions seen in functional connectivity MRI data remain unclear.<sup>54</sup> Tubers could act as spike generators, increasing local activity that leads to suppression of the globi pallidi and vermis. Conversely, tubers could act as lesions, decreasing local activity, leading to increased activity in the connected structure. Alternatively, activity in the globi pallidi or vermis could influence cortical excitability at tuber locations. Future work is needed to better understand the link between tuber locations associated with infantile spasms, the globi pallidi, and the vermis.

### Limitations

First, we have primarily used a normative young adult group connectome ( $n = 1,000$ , age = 18–35 years) to study the connectivity patterns for lesion network mapping.<sup>31</sup> This provides significant signal-to-noise advantages, allows for technique standardization, and has been highly informative.<sup>16–21</sup> Although this does provide a true indication of the developmental endpoints of connectivity between brain regions, it ignores age-related differences in connectivity that may be important here. However, a large high-quality functional connectivity dataset from ~2–3-year-old children is not currently available, and a direct test of lesion network mapping using an age-matched connectome is not yet feasible. Nevertheless, we have thus far seen minimal impact from methodological differences in how one processes connectome data, for example, global signal regression versus other artifact removal strategies,<sup>16,54</sup> or using patient-specific, age-matched, or disease-matched normative connectomes,<sup>16,55–58</sup> which is reflected here by the consistent localization of infantile spasm-related connections using data from the ABCD 9-year-old group connectome ( $n = 1,000$ ; see Fig 4E vs Fig 4F). It is possible that our results could be improved by using a connectome better matched to the age of the TSC patients, and this is an experiment we intend to perform once such data become available and extensively processed given the significant confounds present in young child fMRI data.

Second, lesion network mapping has primarily been used to study lesion-induced disorders in previously healthy participants<sup>20</sup>; however, tubers are congenital, affecting the maturation of developing brain networks.<sup>59</sup>

We argue, however, that disruption of the local architecture drives the (partial) transfer of functions originally destined to be in those affected areas, and that the dysplastic neurons in tubers generate abnormal activity locally.<sup>45</sup>

Finally, the goal of the present study was to test whether tuber distributions associated with spasms map to a common brain network, to define this network, and to assess the consistency of this network. Whether tuber distributions associated with spasms directly correlate with functional connectivity differences in these same children is a topic we intend to pursue.<sup>59</sup> It is impossible, however, to delineate which of this altered connectivity represents causation, compensation, or downstream effects from infantile spasms. Because the presence, location, and extent of cortical tubers is consistent before and after the onset of spasms, we believe the presented analysis is more likely to represent causal information.

### Conclusions

In summary, our results provide evidence for the location of key network nodes for a potential infantile spasms network, but further work is needed to understand the specific pathophysiology at these locations. We propose that future efforts to clarify the role these structures play in spasmogenesis via pallidal and vermian GABAergic knockout models and depth electrode studies, as well as comparison of the results presented here with cortical tuber resection outcomes and EEG source localization, will also clarify the clinical implications of the presented results. Furthermore, lesion network mapping of individual tuber lesions rather than lesion patterns in patients with available EEG data may identify spasmogenic tubers, leading to an approach for candidate selection for epilepsy surgery or noninvasive brain stimulation.

At present, we have a moderate predictive ability to identify those at elevated risk for infantile spasms in TSC. Looking forward, refinement of this predictive model with the inclusion of serial EEG data and EEG connectivity metrics will likely enhance its performance.<sup>60,61</sup> Additionally, preventative treatment of seizures with vigabatrin is currently being studied for TSC in Europe<sup>62</sup> and the United States (NCT02849457). Specific prediction of spasms based on our imaging methods may allow for improved risk stratification and limit exposure to vigabatrin for pre-emptive treatment to those at higher risk.

### Acknowledgments

This research was supported by awards from multiple NIH grants including NINDS U01NS082320 (M.S. and D.A.K.), NIMH T32MH112510 and NIMH K23MH120510 (A.L.C. and P.M.), NINDS U54NS092090 (M.S.), NICHD

U54HD090255 (M.S.), and NINDS K23NS083741 (M.F.), as well as funding from the TS Alliance to TACERN, the Child Neurology Foundation (A.L.C. and M.R.K.), the Sidney R. Baer, Jr. Foundation (M.F.), the Dystonia Foundation (M.F.), and the Nancy Lurie Marks Foundation (M.F.).

We are sincerely indebted to the generosity of the families and patients in TSC clinics across the United States who contributed their time and effort to this study. We also thank the Tuberous Sclerosis Alliance for its continued support of TSC research.

## Genomics Superstruct Project (GSP) Acknowledgments

Data were provided (in part) by the Brain Genomics Superstruct Project of Harvard University and Massachusetts General Hospital (principal investigators: Randy Buckner, Joshua Roffman, and Jordan Smoller), with support from the Center for Brain Science Neuroinformatics Research Group, the Athinoula A. Martinos Center for Biomedical Imaging, and the Center for Human Genetic Research. Twenty individual investigators at Harvard University and Massachusetts General Hospital generously contributed data to the overall project.

## Adolescent Brain Cognitive Development (ABCD) Acknowledgments

Some of the data used in the preparation of this article were obtained from the ABCD study (<https://abcdstudy.org>), held in the National Institute of Mental Health Data Archive. This is a multisite, longitudinal study designed to recruit more than 10,000 children aged 9–10 years and follow them over 10 years into early adulthood. The ABCD study is supported by the NIH and additional federal partners under award numbers U01DA041048, U01DA050989, U01DA051016, U01DA041022, U01DA051018, U01DA051037, U01DA050987, U01DA041174, U01DA041106, U01DA041117, U01DA041028, U01DA041134, U01DA050988, U01DA051039, U01DA041156, U01DA041025, U01DA041120, U01DA051038, U01DA041148, U01DA041093, U01DA041089, U24DA041123, U24DA041147. A full list of supporters is available at <https://abcdstudy.org/federal-partners.html>. A listing of participating sites and a complete listing of the study investigators can be found at <https://abcdstudy.org/scientists/workgroups/>. ABCD consortium investigators designed and implemented the study and/or provided data but did not necessarily participate in analysis or writing of this report. This article reflects the views of the authors and may not

reflect the opinions or views of the NIH or ABCD consortium investigators. The ABCD data repository grows and changes over time. The ABCD data used in this report are listed at: <https://nda.nih.gov/study.html?id=1054>, doi: 10.15154/1520630.

## Author Contributions

A.L.C., B.P.F.M., M.F., M.S., D.A.K., J.Y.W., E.M.B., H.N., S.K.W., and J.M.P. contributed to the conception and design of the study; all authors contributed to the acquisition and analysis of data; A.L.C., B.P.F.M., M.F., and J.M.P. contributed to drafting a significant portion of the text and preparing the figures. Members of the TACERN group that contributed data for this project are listed in the supplementary online Table S1.

## Potential Conflicts of Interest

Nothing to report.

## References

- Osborne JP, Fryer A, Webb D. Epidemiology of tuberous sclerosis. *Ann N Y Acad Sci* 1991;615:125–127.
- Peters JM, Prohl AK, Tomas-Fernandez XK, et al. Tubers are neither static nor discrete. *Neurology* 2015;85:1536–1545.
- Liang S, Zhang J, Yang Z, et al. Long-term outcomes of epilepsy surgery in tuberous sclerosis complex. *J Neurol* 2017;264:1146–1154.
- Davis PE, Filip-Dhima R, Sideridis G, et al. Presentation and diagnosis of tuberous sclerosis complex in infants. *Pediatrics* 2017; 140:1–11.
- Chu-Shore CJ, Major P, Camposano S, et al. The natural history of epilepsy in tuberous sclerosis complex. *Epilepsia* 2010;51: 1236–1241.
- Osborne JP, Edwards SW, Dietrich Alber F, et al. The underlying etiology of infantile spasms (West syndrome): information from the International Collaborative Infantile Spasms Study (ICISS). *Epilepsia* 2019;60:1861–1869.
- Bolton PF, Griffiths PD. Association of tuberous sclerosis of temporal lobes with autism and atypical autism. *Lancet* 1997;349:392–395.
- Bolton PF, Park RJ, Higgins JNP, et al. Neuro-epileptic determinants of autism spectrum disorders in tuberous sclerosis complex. *Brain* 2002;125:1247–1255.
- Numis AL, Major P, Montenegro MA, et al. Identification of risk factors for autism spectrum disorders in tuberous sclerosis complex. *Neurology* 2011;76:981–987.
- Mous SE, Overwater IE, Vidal Gato R, et al. Cortical dysplasia and autistic trait severity in children with tuberous sclerosis complex: a clinical epidemiological study. *Eur Child Adolesc Psychiatry* 2018;27: 753–765.
- Walz NC, Byars AW, Egelhoff JC, Franz DN. Supratentorial tuber location and autism in tuberous sclerosis complex. *J Child Neurol* 2002;17:830–832.
- Ridler K, Suckling J, Higgins N, et al. Standardized whole brain mapping of tubers and subependymal nodules in tuberous sclerosis complex. *J Child Neurol* 2004;19:658–665.

13. Harini C, Sharda S, Bergin AM, et al. Detailed magnetic resonance imaging (MRI) analysis in infantile spasms. *J Child Neurol* 2018;33:405–412.
14. Jansen FE, Vincken KL, Algra A, et al. Cognitive impairment in tuberous sclerosis complex is a multifactorial condition. *Neurology* 2008;70:916–923.
15. Rorden C, Karnath HO, Bonilha L. Improving lesion-symptom mapping. *J Cogn Neurosci* 2007;19:1081–1088.
16. Boes AD, Prasad S, Liu H, et al. Network localization of neurological symptoms from focal brain lesions. *Brain* 2015;138:3061–3075.
17. Darby RR, Laganier S, Pascual-Leone A, et al. Finding the imposter: brain connectivity of lesions causing delusional misidentifications. *Brain* 2017;140:497–507.
18. Darby RR, Horn A, Cushman F, Fox MD. Lesion network localization of criminal behavior. *Proc Natl Acad Sci U S A* 2018;115:601–606.
19. Cohen AL, Soussand L, Corrow SL, et al. Looking beyond the face area: lesion network mapping of prosopagnosia. *Brain* 2019;142:3975–3990.
20. Fox MD. Mapping symptoms to brain networks with the human connectome. *N Engl J Med* 2018;379:2237–2245.
21. Joutsa J, Shih LC, Horn A, et al. Identifying therapeutic targets from spontaneous beneficial brain lesions. *Ann Neurol* 2018;84:153–157.
22. Hashemi SR, Salehi SSM, Erdogmus D, et al. Asymmetric loss functions and deep densely-connected networks for highly-imbalanced medical image segmentation: application to multiple sclerosis lesion detection. *IEEE Access* 2019;7:1721–1735.
23. Yushkevich P, Piven J, Cody H, Ho S. User-guided level set segmentation of anatomical structures with ITK-SNAP. *Neuroimage* 2006;31:1116–1128.
24. Andersen SM, Rapcsak SZ, Beeson PM. Cost function masking during normalization of brains with focal lesions: still a necessity? *Neuroimage* 2010;53:78–84.
25. Winkler AM, Ridgway GR, Webster MA, et al. Permutation inference for the general linear model. *Neuroimage* 2014;92:381–397.
26. Sperber C, Karnath HO. Impact of correction factors in human brain lesion-behavior inference. *Hum Brain Mapp* 2017;38:1692–1701.
27. Ge T, Müller-Lenke N, Bendfeldt K, et al. Analysis of multiple sclerosis lesions via spatially varying coefficients. *Ann Appl Stat* 2014;8:1095–1118.
28. Mazziotta J, Toga A, Evans A, et al. A probabilistic atlas and reference system for the human brain: International Consortium for Brain Mapping (ICBM). *Philos Trans R Soc Lond B Biol Sci* 2001;356:1293–1322.
29. Thomas Yeo BT, Krienen FM, Sepulcre J, et al. The organization of the human cerebral cortex estimated by intrinsic functional connectivity. *J Neurophysiol* 2011;106:1125–1165.
30. Abraham A, Pedregosa F, Eickenberg M, et al. Machine learning for neuroimaging with scikit-learn. *Front Neuroinform* 2014;8:14.
31. Cohen AL, Fox MD. Reply: The influence of sample size and arbitrary statistical thresholds in lesion-network mapping. *Brain* 2020;143:e41.
32. Eklund A, Nichols TE, Knutsson H. Cluster failure: why fMRI inferences for spatial extent have inflated false-positive rates. *Proc Natl Acad Sci U S A* 2016;113:7900–7905.
33. Volkow ND, Koob GF, Croyle RT, et al. The conception of the ABCD study: from substance use to a broad NIH collaboration. *Dev Cogn Neurosci* 2018;32:4–7.
34. Fischl B. FreeSurfer. *Neuroimage* 2012;62:774–781.
35. Li J, Kong R, Liégeois R, et al. Global signal regression strengthens association between resting-state functional connectivity and behavior. *Neuroimage* 2019;196:126–141.
36. Seabold S, Perktold J. Statsmodels: econometric and statistical modeling with Python. *Proceedings of the 9th Python in Science Conference*. 2010. Available at: <http://conference.scipy.org/proceedings/scipy2010/pdfs/seabold.pdf>. Accessed February 2, 2019.
37. Pedregosa F, Varoquaux G, Gramfort A, et al. Scikit-learn: machine learning in Python. *J Mach Learn Res* 2011;12:2825–2830.
38. Baron RM, Kenny DA. The moderator–mediator variable distinction in social psychological research: conceptual, strategic, and statistical considerations. *J Pers Soc Psychol* 1986;51:1173–1182.
39. Hayes AF. *Introduction to mediation, moderation, and conditional process analysis. A regression-based approach*. 2nd ed. New York, NY: Guilford Publications, 2017.
40. Bolton PF, Clifford M, Tye C, et al. Intellectual abilities in tuberous sclerosis complex: risk factors and correlates from the Tuberous Sclerosis 2000 Study. *Psychol Med* 2015;45:2321–2331.
41. Doherty C, Goh S, Poussaint TY, et al. Prognostic significance of tuber count and location in tuberous sclerosis complex. *J Child Neurol* 2005;20:837–841.
42. van Eeghen AM, Pulsifer MB, Merker VL, et al. Understanding relationships between autism, intelligence, and epilepsy: a cross-disorder approach. *Dev Med Child Neurol* 2013;55:146–153.
43. Meikle L, Talos DM, Onda H, et al. A mouse model of tuberous sclerosis: neuronal loss of Tsc1 causes dysplastic and ectopic neurons, reduced myelination, seizure activity, and limited survival. *J Neurosci* 2007;27:5546–5558.
44. Lado FA, Moshé SL. Role of subcortical structures in the pathogenesis of infantile spasms: what are possible subcortical mediators? *Int Rev Neurobiol* 2002;49:115–140.
45. Chugani HT, Ilyas M, Kumar A, et al. Surgical treatment for refractory epileptic spasms: the Detroit series. *Epilepsia* 2015;56:1941–1949.
46. Jacobs J, Rohr A, Moeller F, et al. Evaluation of epileptogenic networks in children with tuberous sclerosis complex using EEG-fMRI. *Epilepsia* 2008;49:816–825.
47. Chugani HT, Shewmon DA, Sankar R, et al. Infantile spasms: II. Lenticular nuclei and brain stem activation on positron emission tomography. *Ann Neurol* 1992;31:212–219.
48. Wycis HT, Baird HW, Spiegel EA. Long range results following pallidotomy and pallidoamygdalotomy in certain types of convulsive disorders. *Stereotact Funct Neurosurg* 1966;27:114–120.
49. Uusisaari M, Knöpfel T. GABAergic synaptic communication in the GABAergic and non-GABAergic cells in the deep cerebellar nuclei. *Neuroscience* 2008;156:537–549.
50. Pearl PL, Vezina LG, Saneto RP, et al. Cerebral MRI abnormalities associated with vigabatrin therapy. *Epilepsia* 2009;50:184–194.
51. Desguerre I, Marti I, Valayannopoulos V, et al. Transient magnetic resonance diffusion abnormalities in West syndrome: the radiological expression of non-convulsive status epilepticus? *Dev Med Child Neurol* 2008;50:112–116.
52. Sutoo D, Akiyama K, Yabe K. Quantitative maps of GABAergic and glutamatergic neuronal systems in the human brain. *Hum Brain Mapp* 2000;11:93–103.
53. Scantlebury MH, Galanopoulou AS, Chudomelova L, et al. A model of symptomatic infantile spasms syndrome. *Neurobiol Dis* 2010;37:604–612.
54. Murphy K, Fox MD. Towards a consensus regarding global signal regression for resting state functional connectivity MRI. *Neuroimage* 2017;154:169–173.
55. Horn A, Reich M, Vorwerk J, et al. Connectivity predicts deep brain stimulation outcome in Parkinson disease. *Ann Neurol* 2017;82:67–78.
56. Weigand A, Horn A, Caballero R, et al. Prospective validation that subgenual connectivity predicts antidepressant efficacy of transcranial magnetic stimulation sites. *Biol Psychiatry* 2018;84:28–37.



57. Cash RFH, Zalesky A, Thomson RH, et al. Subgenual functional connectivity predicts antidepressant treatment response to transcranial magnetic stimulation: independent validation and evaluation of personalization. *Biol Psychiatry* 2019;86:e5–e7.
58. Wang Q, Akram H, Muthuraman M, et al. Normative vs patient-specific brain connectivity in deep brain stimulation. *Neuroimage* 2021;224:117307.
59. Im K, Ahtam B, Haehn D, et al. Altered structural brain networks in tuberous sclerosis complex. *Cereb Cortex* 2016;26:2046–2058.
60. Wu JY, Goyal M, Peters JM, et al. Scalp EEG spikes predict impending epilepsy in TSC infants: a longitudinal observational study. *Epilepsia* 2019;60:2428–2436.
61. Davis PE, Kapur K, Filip-Dhima R, et al. Increased electroencephalography connectivity precedes epileptic spasm onset in infants with tuberous sclerosis complex. *Epilepsia* 2019;60:1721–1732.
62. Kotulska K, Kwiatkowski DJ, Curatolo P, et al. Prevention of epilepsy in infants with tuberous sclerosis complex in the EPISTOP trial. *Annals of Neurology*. 2021;89:304–314. <http://dx.doi.org/10.1002/ana.25956>.